Application of the Mode Matching Technique for the Computation of the Beam Parameters of an Infinite Periodic Structure

A. Jöstingmeier, M. Dohlus and N. Holtkamp

Deutsches Elektronen-Synchrotron DESY
Gruppe Beschleunigerphysik
Notkestr. 85, D-22607 Hamburg, Germany

Abstract

In this contribution, the mode matching technique is employed for the computation of the beam impedance, the wakefield and the loss parameter of a planar infinite periodic structure. It is shown that such a grating may also be used as a model for a corrugated circular beampipe if the parameters of the planar structure are properly chosen. Furthermore it is demonstrated how the Rayleigh expansion which is used for the field representation above the grating has to be modified if we consider an ultra-relativistic beam. Numerical results are presented for various examples. The validity of the mode matching technique is examined by comparing the wakefields which are calculated using the proposed method and the MAFIA computer code.

I. Introduction

Periodic structures play an important role in the field of linear accelerators. Fig. 1 presents two examples: The accelerating structure itself shown in Fig. 1(a) is a periodic structure. Secondly, Fig. 1(b) shows the longitudinal section of a higher order mode absorber which has recently been proposed for TESLA [1], [2]. This absorber consists of a stack of about 250 parallel-plate waveguides which is accomodated in a pillbox-like cavity. The parallel-plate waveguides are used to extract the higher order mode from the beampipe and to attenuate the high frequency spectral components of the extracted field by the surface losses of the metal slabs. On the other hand, the additional absorbing material at the outer radius of the absorber is necessary in order to suppress low frequency long range wakefields which are not sufficiently damped by the ohmic losses of the waveguides.

For beam dynamics simulations it is important to know the beam impedance, the wakefield and the loss parameter for such periodic structures. Therefore much effort has already been made in order to investigate this kind of problems. In several papers dealing with periodic structures the high-frequency limit of the beam impedance has been studied. For example, this quantity has been investigated in detail for a periodic array of cylindrically symmetric cavities connected by beampipes and for an array of infinitely thin diaphragms in a circular pipe in [3] and [4], respectively. The analysis presented in [3] leads to some important scaling laws for the beam impedance. Among other things, it has been demonstrated in [3] that the beam impedance of an infinite periodic structure is proportional to $\omega^{-3/2}$ for high frequencies.

In this contribution, the mode matching technique [5]-[7] is used in order to calculate the electromagnetic field which is excited by an ultra-relativistic bunch of particles in the presence

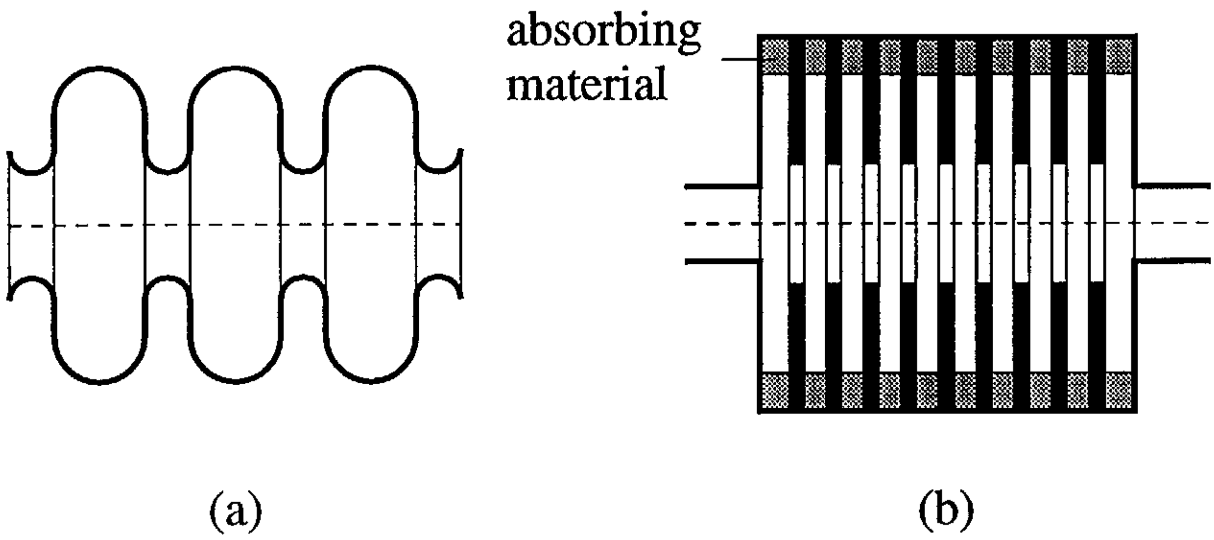

Figure 1: Two examples for periodic structures. (a) Sketch of an accelerating structure. (b) Schematic drawing of a proposal for a higher order mode absorber for TESLA.

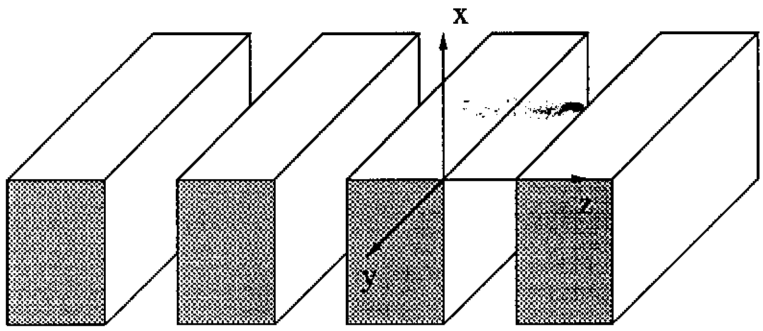

Figure 2: Planar grating consisting of an infinite number of parallel-plate waveguides.

of an infinite periodic structure. Subsequently, the beam parameters are calculated by making use of the results of the field analysis. Except for the limited computer resources, there are no other principal limitations for the accuracy of the method. Furthermore the numerical efficiency of the presented method is quite high. Therefore it is especially useful if very short bunches are considered for which we need to know the beam impedance over a broad frequency range.

Since the field analysis of a planar structure is much easier than that of a circular configuration we apply the mode matching technique to an infinite array of parallel-plate waveguides which is shown in Fig. 2. The electromagnetic field of this structure is independent of the y-coordinate. However, most of the relevant examples for periodic structures are circular symmetric. Therefore we analytically calculate the beam impedances corresponding to a circular and a planar two-layer problem in order to demonstrate that the planar structure can be used as a model for the circular one if the parameters describing the structures obey certain relations.

The electromagnetic properties of a grating and a dielectric layer are very close to each other as long as the free-space wavelength is larger than the grating period [8]. For this frequency range it can hence be concluded that a circular corrugated beampipe is equivalent to a planar grating if the same parameter relations are fulfilled as for the two-layer problems. For higher frequencies the behaviour of a dielectric layer and a grating becomes different. Nevertheless, it is evident that the beam impedances of a circular corrugated beampipe and a planar grating are the same if the curvature of the circular structure can be neglected over one wavelength.

If we use the parallel-plate waveguide model for an accelerating structure according to Fig. 1(a), it is clear that we have to short-circuit the waveguides at a certain depth. On the other hand, the parallel-plate waveguides are more or less matched in the case of the TESLA absorber shown in Fig. 1(b) due to the absorbing material. In principle it makes no difference for the mode matching technique how the waveguides are terminated.

Since we are basically interested in the short range wake, and because the distance between the waveguide termination and the grating interface is in general much larger than the bunch length, an arbitrary load may be assumed. It is worth noting that the beam impedance does depend on the waveguide termination. Nevertheless, the short range wake and the loss parameter are independent of it for bunches which are shorter than the distance between the load and the grating interface. For the sake of simplicity we choose a matched load corresponding to parallel-plate waveguides which extend to $-\infty$ with respect to the x-direction.

Practical structures always have a finite length. Thus a criterion is required which allows us to decide whether the length of a structure is sufficiently large so that it can be considered as infinite. This problem has already been discussed in many publications as e.g. in [9], [10]. It has been found that the so-called critical length which is used to describe the transition between the single cell solution and that corresponding to the infinite periodic structure is proportional to the aperture radius squared divided by the bunch length. Hence, we have to keep in mind that the critical length becomes large for short bunches.

II. Relation between a planar and a circular two-layer problem

In the following two subsections, we consider a circular and a planar two-layer problem illustrated in Figs. 3 and 4, respectively, in order to show the equivalence between the two structures. Note that the second layer extends to infinity in Figs. 3 and 4. For both of these two-layer problems, we obtain an analytic expression for the beam impedance so that the conditions under which both configurations are equivalent can easily be established.

The circular two-layer problem consists of the cylindrically symmetric structure. Region (1) ($\rho \leq a$) is characterized by a permittivity equal to that of free-space whereas region (2) ($\rho > a$) has a relative permittivity of ε_r. The azimuthally independent electromagnetic field is excited by a current I_0 flowing along the z-coordinate. This configuration is compared with the planar structure of Fig. 4 which is excited by a y-independent surface current J_s backed by a magnetic wall. This boundary condition has to be enforced in order to make both configurations comparable for the following reason: Both E_ρ and H_φ vanish at the center of the circular structure. Since E_x and H_y of the planar problem correspond to E_ρ and H_φ, respectively, it is evident that these field components must also vanish at $x = d$ if both configurations should be equivalent which is just guaranteed by the magnetic wall.

IIa) Planar two-layer problem

In the frequency domain, the surface current density $\boldsymbol{J}_s$ is proportional to $e^{-jk_0 z}$ for an ultra-

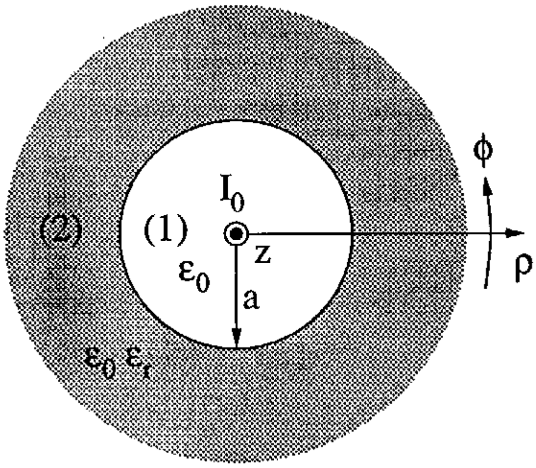

Figure 3: Circular two-layer problem.

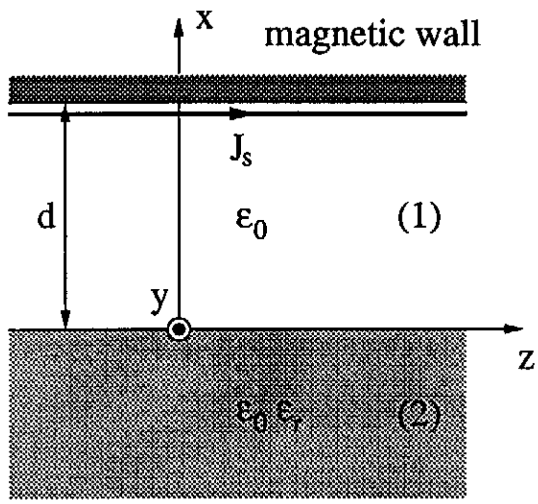

Figure 4: Planar two-layer problem.

relativistic beam where k_0 denotes the vacuum wavenumber. Thus $\boldsymbol{J}_s$ can be written as

$$\boldsymbol{J}_s = J_{sz} e^{-jk_0 z} \hat{\boldsymbol{e}}_z \quad . \tag{1}$$

The quantities $\hat{\boldsymbol{e}}_z$ and J_{sz} are the unit vector in the z-direction and the amplitude of the surface current density.

Due to the symmetry of the structure only three components of the electromagnetic field are excited, namely, E_x, E_z and H_y. Let us start the analysis with the wave equation for H_y in region (1) which reads

$$\left(\frac{\partial^2}{\partial x^2} + \frac{\partial^2}{\partial z^2}\right) H_y^{(1)} + k_0^2 H_y^{(1)} = 0 \quad . \tag{2}$$

The electromagnetic field has obviously the same z-dependence as $\boldsymbol{J}_s$ which in particular means that

$$H_y^{(1)} \propto e^{-jk_0 z} \quad . \tag{3}$$

Inserting this relation into the wave equation immediately yields

$$\frac{\partial^2}{\partial x^2} H_y^{(1)} = 0 \quad . \tag{4}$$

Consequently, $H_y^{(1)}$ is given by

$$H_y^{(1)} = \left(A \frac{d-x}{d} + B\right) e^{-jk_0 z} \quad , \tag{5}$$

where A and B are integration constants to be determined. Using the equation $\nabla \times \boldsymbol{H}^{(1)} = j\omega\varepsilon_0 \boldsymbol{E}^{(1)}$, we obtain for the z-component of the electric field

$$E_z^{(1)} = \frac{Z_0}{jk_0} \frac{\partial H_y^{(1)}}{\partial x} = -A Z_0 \frac{1}{jk_0 d} e^{-jk_0 z} \quad . \tag{6}$$

The integration constant B can be eliminated by making use of the boundary condition for $H_y^{(1)}$ at $x = d$ which is

$$H_y^{(1)}\Big|_{x=d} = -J_{sz}e^{-jk_0 z} \quad . \tag{7}$$

Substituting the general solution for $H_y^{(1)}$ from Eq. (5) into the boundary condition (7), we obtain

$$B = -J_{sz} \tag{8}$$

The electromagnetic field in region (2) is given by a plane wave:

$$H_y^{(2)} = Ce^{-j(k_0 z - \beta x)} \quad , \tag{9}$$

where C and β denote the amplitude of this wave and its propagation factor in the negative x-direction. According to the separation condition, β reads

$$\beta = \sqrt{\varepsilon_r k_0^2 - k_0^2} = k_0\sqrt{\varepsilon_r - 1} \quad . \tag{10}$$

By making use of $\nabla \times \boldsymbol{H}^{(2)} = j\omega\varepsilon_0\varepsilon_r \boldsymbol{E}^{(2)}$, we get for the z-component of the electric field in region (2)

$$E_z^{(2)} = \frac{Z_0}{j\varepsilon_r k_0}\frac{\partial H_y^{(2)}}{\partial x} = CZ_0\frac{\beta}{\varepsilon_r k_0}e^{-j(k_0 z - \beta x)} \quad . \tag{11}$$

The unknowns A and C can now be calculated by exploiting the continuity conditions at $x = 0$ which are

$$H_y^{(1)}\Big|_{x=0} = H_y^{(2)}\Big|_{x=0} \quad , \tag{12}$$

$$E_z^{(1)}\Big|_{x=0} = E_z^{(2)}\Big|_{x=0} \quad . \tag{13}$$

For the sake of clarity let us define the impedance $Z_p^{(2)}$ which is given by the ratio of $E_z^{(2)}$ and $H_y^{(2)}$ at $x = 0$:

$$Z_p^{(2)} = \frac{E_z^{(2)}}{H_y^{(2)}}\Bigg|_{x=0} = \frac{\beta}{\varepsilon_r k_0}Z_0 = \frac{\sqrt{\varepsilon_r - 1}}{\varepsilon_r}Z_0 \tag{14}$$

Note that this impedance is not the wave impedance of a plane wave in medium (2) which is just $Z_0/\sqrt{\varepsilon_r}$. Taking the definition of $Z_p^{(2)}$ into account, we can rewrite the continuity condition (13):

$$E_z^{(1)}\Big|_{x=0} = Z_p^{(2)} H_y^{(2)}\Big|_{x=0} \tag{15}$$

Inserting the field representations from Eqs. (5),(6) and (9) into the continuity conditions (12) and (15), we obtain for the integration constant A:

$$A = \frac{J_{sz}}{1 + \dfrac{Z_0}{jk_0 d Z_p^{(2)}}} \tag{16}$$

With A according to the above equation we arrive at the following expression for the beam impedance of the planar two-layer problem:

$$Z_p^b = \frac{E_z^{(1)}\Big|_{x=0}}{J_{sz}} = -\frac{Z_0}{jk_0 d + \dfrac{Z_0}{Z_p^{(2)}}} \tag{17}$$

It is worth noting that for high frequencies with $k_0 d \gg Z_0/Z_p^{(2)}$ the beam impedance can be approximated by

$$Z_p^b \approx -\frac{Z_0}{jk_0 d} \quad . \tag{18}$$

This means that Z_p^b does not depend on the material properties of the dielectric layer in this frequency range.

It is also interesting to examine the limit of Z_p^b for $k_0 \to 0$ which amounts to

$$\lim_{k_0 \to 0} Z_p^b = -\frac{\sqrt{\varepsilon_r - 1}}{\varepsilon_r} Z_0 \quad . \tag{19}$$

Note that the beam impedance of a planar structure is real and does not vanish in the dc case.

IIb) Circular two-layer problem

In the circular configuration the current I along the z-axis is given by

$$I = I_0 e^{-jk_0 z} \quad , \tag{20}$$

where I_0 denotes the amplitude of I. Similar to the planar structure only three components of the electromagnetic field are excited by I which are E_ρ, E_z and H_φ. After eliminating E_ρ and E_z from Maxwell's equation, it is found that the azimuthal component of the magnetic field in region (1) $H_\varphi^{(1)}$ satisfies the equation

$$\frac{\partial}{\partial \rho}\frac{1}{\rho}\frac{\partial\left(\rho H_\varphi^{(1)}\right)}{\partial \rho} + \frac{\partial^2 H_\varphi^{(1)}}{\partial z^2} + k_0^2 H_\varphi^{(1)} = 0 \quad . \tag{21}$$

Note that the former differential equation is not Bessel's equation. The general solution of Eq. (21) reads

$$H_\varphi^{(1)} = \left(A\rho + \frac{B}{\rho}\right) e^{-jk_0 z} \quad , \tag{22}$$

where A and B are integration constants which are to be determined by the continuity conditions at $\rho = 0$ and $\rho = a$. By making use of $\boldsymbol{\nabla} \times \boldsymbol{H}^{(1)} = j\omega\varepsilon_0 \boldsymbol{E}^{(1)}$ in cylindrical coordinates, we get for the axial component of the electric field in region (1)

$$E_z^{(1)} = \frac{Z_0}{jk_0\rho}\frac{\partial\left(\rho H_\varphi^{(1)}\right)}{\partial \rho} = \frac{Z_0}{jk_0} 2A e^{-jk_0 z} \quad . \tag{23}$$

The coefficient B can be calculated by invoking Ampere's law:

$$\lim_{\rho \to 0} \oint_{C_\rho} H_\varphi^{(1)} \rho \, d\varphi = I_0 e^{-jk_0 z} \tag{24}$$

Insertion of $H_\varphi^{(1)}$ from Eq. (22) into the previous equation yields

$$B = \frac{I_0}{2\pi} \quad . \tag{25}$$

The wavenumber of the electromagnetic field in region (2) is $\sqrt{\varepsilon_r}k_0$. Thus the axial component of the electric field in this region fulfills

$$\frac{1}{\rho}\frac{\partial}{\partial\rho}\rho\frac{\partial E_z^{(2)}}{\partial\rho} + (\varepsilon_r - 1)\,k_0^2 E_z^{(2)} = 0 \tag{26}$$

which is just Bessel's equation. The solution of Eq. (26) is a radially outward travelling wave which can be written as

$$E_z^{(2)} = C\mathrm{H}_0^{(2)}(k_t\rho)\,e^{-jk_0 z} \quad , \tag{27}$$

where C and $\mathrm{H}_0^{(2)}$ are the still unknown amplitude of this wave and the zeroth order Hankel function of second kind. The transverse wavenumber k_t is equal to the phase factor β of Eq. (10):

$$k_t = \beta = k_0\sqrt{\varepsilon_r - 1} \tag{28}$$

After some straightforward manipulations we obtain

$$H_\varphi^{(2)} = \frac{1}{jk_0 Z_0}\frac{1}{1-\dfrac{1}{\varepsilon_r}}Ck_t\mathrm{H}_0^{(2)\prime}(k_t\rho)\,e^{-jk_0 z} \tag{29}$$

for the azimuthal magnetic field in medium (2).

Before we make use of the continuity conditions at $\rho = a$, let us introduce an impedance $Z_c^{(2)}$ which is equivalent to $Z_p^{(2)}$ of Eq. (14). The impedance $Z_p^{(2)}$ is defined as the ratio of $E_z^{(2)}$ and $H_y^{(2)}$ so that the Poynting vector which corresponds to these field components is directed along the negative x-direction. Therefore $Z_c^{(2)}$ is defined such that the corresponding Poynting vector is outward directed (in the positive ρ-direction):

$$Z_c^{(2)} = -\left.\frac{E_z^{(2)}}{H_\varphi^{(2)}}\right|_{\rho=a} \tag{30}$$

Inserting Eqs. (27), (28) and (29) into Eq. (30) and keeping in mind that $\mathrm{H}_0^{(2)\prime}(k_t a) = -\mathrm{H}_1^{(2)}(k_t a)$ leads to

$$Z_c^{(2)} = j\frac{\mathrm{H}_0^{(2)}(k_t a)}{\mathrm{H}_1^{(2)}(k_t a)}\frac{\sqrt{\varepsilon_r - 1}}{\varepsilon_r}Z_0 \quad . \tag{31}$$

If we exploit the continuity conditions at $\rho = a$ which are

$$\left.E_z^{(1)}\right|_{\rho=a} = \left.E_z^{(2)}\right|_{\rho=a} \quad , \tag{32}$$

$$\left.H_\varphi^{(1)}\right|_{\rho=a} = \left.H_\varphi^{(2)}\right|_{\rho=a} \quad , \tag{33}$$

we get for the integration constant A

$$A = -\frac{I_0}{4\pi a}\frac{jk_0}{jk_0\dfrac{a}{2} + \dfrac{Z_0}{Z_c^{(2)}}} \quad . \tag{34}$$

Let us define the impedance Z_c^b as the ratio of $E_z^{(1)}$ at $\rho = a$ to $I_0/(2\pi a/2)$. The latter quantity represents the surface current density if we uniformly distribute the current I_0 over the circumference of a circle with the radius $a/2$. Substituting the expression for A according to Eq. (34) into Eq. (23), we obtain for Z_c^b

$$Z_c^b = \frac{E_z^{(1)}\Big|_{\rho=0}}{\dfrac{I_0}{2\pi a/2}} = -\frac{1}{2}\frac{Z_0}{jk_0\dfrac{a}{2} + \dfrac{Z_0}{Z_c^{(2)}}} \quad . \tag{35}$$

From the asymptotic behaviour of the Hankel functions [11] which is

$$\mathrm{H}_\nu^{(2)}(x) \rightarrow \sqrt{\frac{2j}{\pi x}} j^\nu e^{-jx} \quad \text{for} \quad x \rightarrow \infty \quad , \tag{36}$$

it is found that the impedances $Z_c^{(2)}$ and $Z_p^{(2)}$ converge to each other for high frequencies:

$$\lim_{k_0 \rightarrow \infty} Z_c^{(2)} = \frac{\sqrt{\varepsilon_r - 1}}{\varepsilon_r} Z_0 = Z_p^{(2)} \tag{37}$$

The large argument approximation of the Hankel functions has also been used in [12] where it is denoted as "plane wall approximation". If we now compare the expressions for Z_c^b and Z_p^b according to Eqs. (35) and (17), respectively, the equivalence between the planar and the circular two-layer problem becomes obvious: Z_c^b is just one half of Z_p^b if we choose the distance between the magnetic wall and the dielectric layer for the planar structure as one half of the radius of the interface between the regions (1) and (2) of the circular structure. Thus we can use the planar configuration as a model for the circular one if we take into account the corresponding scaling laws. Furthermore the agreement between the two models becomes better, the higher the considered frequency is.

Nevertheless, it is also interesting to investigate low frequencies. If the considered frequency is low but the large argument approximation of the Hankel functions is still valid we get for the beam impedance of the circular configuration

$$2Z_c^b = \frac{E_z^{(1)}\Big|_{\rho=0}}{\dfrac{I_0}{2\pi a}} = -Z_p^{(2)} \quad \text{for} \quad \frac{k_0 a}{2} \ll \frac{\varepsilon_r}{\sqrt{\varepsilon_r - 1}} \quad . \tag{38}$$

Comparing the low frequency approximations of the beam impedances of Eqs. (19) and (38), it turns out that Z_p^b equals two times Z_c^b which is nothing else than the axial electric field at $\rho = 0$ divided by the surface current density $I_0/(2\pi a)$. If we consider low frequencies it is consequently more convenient to make use of the equivalence between a circular and a planar structure by setting $a = d$ and distributing I_0 uniformly over the circumference of a circle with the radius a in order to get the surface current density for the planar model.

If we really consider $k_0 \rightarrow 0$ we may use the small argument approximations [11] instead of the large argument approximations for the Hankel functions which are

$$\mathrm{H}_0^{(2)}(x) \rightarrow \quad 1 - j\tfrac{2}{\pi}\ln(x) \qquad \text{for} \quad x \rightarrow 0 \quad , \tag{39}$$

$$\mathrm{H}_1^{(2)}(x) \rightarrow \quad \tfrac{1}{2}x + j\tfrac{2}{\pi}\tfrac{1}{x} \qquad \text{for} \quad x \rightarrow 0 \quad . \tag{40}$$

Inserting the above approximations into Eq. (31) yields that $Z_c^{(2)}$ vanishes for $k_0 \rightarrow 0$. Therefore Z_c^b also vanishes in the dc case according to Eq. (35). Keeping in mind that according to Eq. (19) the beam impedance of a planar structure approaches a real constant which is different from zero for $k_0 \rightarrow 0$, we see that both configurations have a completely different frequency behaviour in the frequency range where the large argument approximations of the Hankel functions cannot be applied.

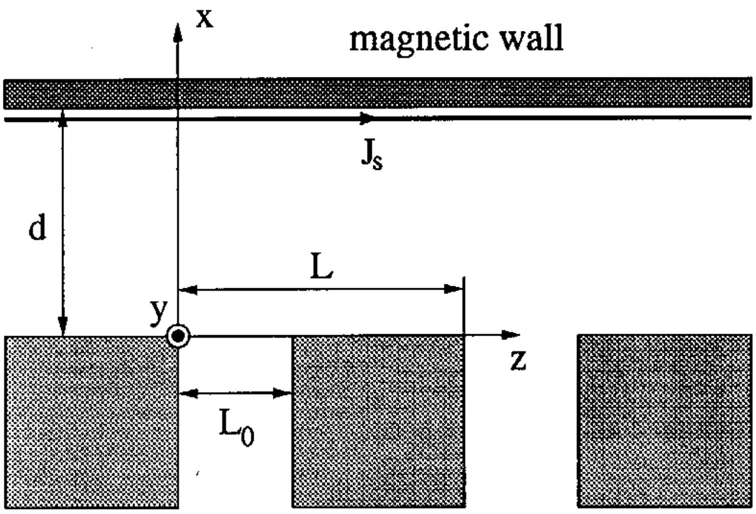

Figure 5: Definition of the grating dimensions.

III. Field analysis of a planar grating

Let us now start with the mode matching analysis of the planar grating with the dimensions which are defined in Fig. 5. The volume density of the exciting current is given by

$$\boldsymbol{J}(x,z,t) = \underbrace{\frac{\Delta q_0}{\Delta y}}_{q_0'} c_0 \delta(x-d)\, f(z-c_0 t)\, \hat{\boldsymbol{e}}_z \quad , \tag{41}$$

where c_0 and q_0' are the velocity of light in vacuum and the charge density per unit length in the y-direction. δ and f denote the Dirac delta-function and the function which desribes the bunch shape along the z-direction. The latter function is normalized according to

$$\int_{\xi=-\infty}^{\infty} f(\xi)\, d\xi = 1 \quad . \tag{42}$$

The mode matching analysis is a frequency domain technique. Hence we make a Fourier transformation of $\boldsymbol{J}(x,z,t)$ yielding

$$\widetilde{\boldsymbol{J}}(x,z,\omega) = \int_{t=-\infty}^{\infty} \boldsymbol{J}(x,z,t)\, e^{-j\omega t} dt = q_0' \delta(x-d)\, \widetilde{f}^*(k_0)\, e^{-jk_0 z} \hat{\boldsymbol{e}}_z \quad , \tag{43}$$

where $\widetilde{f}^*$ denotes the complex conjugate of the Fourier spectrum of f. From now on we distinguish between a time domain quantity and its Fourier transformation by marking the corresponding frequency domain quantity with a "$\sim$". From the boundary condition for the magnetic field at $x = d$ we get

$$\left.\widetilde{H}_y^{(1)}(z,\omega)\right|_{x=d} = -q_0' \widetilde{f}^*(k_0)\, e^{-jk_0 z} \quad . \tag{44}$$

Note that the dimension of $\widetilde{H}_y^{(1)}$ is "(current / length) $*$ time" and not only "current / length" because it is a frequency domain quantity.

For the field representation above the grating ($0 \leq x \leq d$) we make use of the so-called Rayleigh expansion which is just the superposition of the infinite number of spatial harmonics corresponding to the periodic structure. This expansion is known to be complete which means that it can be used to represent any kind of pseudo-periodic field. Nevertheless it must be modified for an ultra-relativistic beam travelling with the speed of light. According to Eq. (43), the phase advance of the exciting current is in this case equal to the vacuum wavenumber which means that the zeroth order spatial harmonic satisfies Eq. (4). Consequently we have to use a constant and a linearly increasing function in the x-direction instead of the zeroth order spatial harmonic of the standard Rayleigh expansion. The field expansion for $0 \leq x \leq d$ finally reads

$$\begin{aligned} \widetilde{H}_y^{(1)}(x,z,\omega) &= \sum_{\substack{n=-\infty \\ n\neq 0}}^{\infty} \mathcal{B}_n \sin(\beta_n (x-d))\, e^{-j\alpha_n z} + \left(-q_0' \widetilde{f}^*(k_0) + a_1 (x-d)\right) e^{-jk_0 z} \quad , && (45) \\ \widetilde{E}_z^{(1)}(x,z,\omega) &= Z_0 \left(\sum_{\substack{n=-\infty \\ n\neq 0}}^{\infty} \mathcal{B}_n \frac{\beta_n}{jk_0} \cos(\beta_n (x-d))\, e^{-j\alpha_n z} + \frac{a_1}{jk_0} e^{-jk_0 z} \right) \quad , && (46) \end{aligned}$$

where the expansion coefficient of the nth harmonic is denoted by $\mathcal{B}_n$; and the phase advance in the z-direction is given by

$$\alpha_n = k_0 - n\frac{2\pi}{L} \quad . \tag{47}$$

For the phase advance in the y-direction we can write according to the separation condition

$$\beta_n = \begin{cases} \sqrt{k_0^2 - \alpha_n^2} & , \quad k_0 \geq \alpha_n \\ -j\sqrt{\alpha_n^2 - k_0^2} & , \quad k_0 < \alpha_n \end{cases} \quad . \tag{48}$$

Note that the representation of $\widetilde{H}_y^{(1)}$ according to Eq. (45) already satisfies the boundary condition (44).

The electromagnetic field within the parallel-plate waveguides is represented in terms of its eigenmodes [13]:

$$\begin{aligned} \widetilde{H}_y^{(2)} &= \sum_{m=0}^{\infty} \mathcal{A}_m \cos(k_{zm} z)\, e^{jk_{xm} x} \quad , && (49) \\ \widetilde{E}_z^{(2)} &= Z_0 \sum_{m=0}^{\infty} \mathcal{A}_m \frac{k_{xm}}{k_0} \cos(k_{zm} z)\, e^{jk_{xm} x} \quad , && (50) \end{aligned}$$

where $\mathcal{A}_m$ is the amplitude of the mth field expansion function and k_{zm} is determined by the height L_0 of the parallel-plate waveguides:

$$k_{zm} = \frac{m\pi}{L_0} \tag{51}$$

Thus the phase advance of the mth waveguide eigenmode in the x-direction reads

$$k_{xm} = \begin{cases} \sqrt{k_0^2 - k_{zm}^2} & , \quad k_0 \geq k_{zm} \\ -j\sqrt{k_{zm}^2 - k_0^2} & , \quad k_0 < k_{zm} \end{cases} \quad . \tag{52}$$

Note that the summation of Eq. (49) starts at $m = 0$ and not at $m = 1$ because the complete set of eigenmodes of a parallel-plate waveguide also includes a TEM mode with respect to the x-direction. This eigenmode which has no x-component of the electric field corresponds to a constant term of a Fourier series.

The still unknown field expansion coefficients $\mathcal{A}_m$ and $\mathcal{B}_n$ of the waveguide modes and the spatial harmonics can be determined from the continuity conditions of the electromagnetic field at the grating interface ($x = d$). The axial component of the diffracted electric field is equal to that of the waveguide field for $0 \le z < L_0$ and vanishes for $L_0 \le z < L$:

$$\tilde{E}_z^{(1)}\Big|_{x=0} = \begin{cases} \tilde{E}_z^{(2)}\Big|_{x=0} & , \quad L_0 \\ 0 & , \quad L - L_0 \end{cases} \tag{53}$$

If we multiply both sides of Eq. (53) by $e^{j\alpha_p z}$ and integrate the resulting equation over one period of the periodic structure we arrive at

$$\sum_{m=0}^{\infty} \mathcal{A}_m \frac{k_{xm}}{k_0} \frac{L_0}{L} C_{pm} = \begin{cases} \dfrac{a_1}{jk_0} & , \quad p = 0 \\ \mathcal{B}_p \dfrac{\beta_p}{jk_0} \cos(\beta_p d) & , \quad p = -\infty, \ldots, -1, +1, \ldots, +\infty \end{cases} \quad , \tag{54}$$

where the coupling integrals C_{pm} are given by

$$C_{pm} = \frac{1}{L_0} \int_{z=0}^{L_0} \cos(k_{zm} z)\, e^{j\alpha_p z} dz \quad . \tag{55}$$

The coupling integrals can be evaluated analytically:

$$C_{pm} = \frac{1}{L_0} \frac{j\alpha_p}{k_{zm}^2 - \alpha_p^2} \left((-1)^m \, e^{j\alpha_p L_0} - 1 \right) \tag{56}$$

For the magnetic field we have the continuity condition

$$\widetilde{H}_y^{(1)}\Big|_{x=0} = \widetilde{H}_y^{(2)}\Big|_{x=0} \quad , \quad L_0 \quad . \tag{57}$$

Multiplying the above equation by the waveguide eigenfunctions and integrating over L_0 we obtain

$$\mathcal{A}_q \frac{1 + \delta_{0q}}{2} = - \sum_{\substack{n=-\infty \\ n \neq 0}}^{\infty} \mathcal{B}_n \sin(\beta_n d)\, C_{nq}^* - \left(q_0' \tilde{f}^*(k_0) + a_1 d \right) C_{0q}^* \quad , \tag{58}$$

where δ_{0q} denotes Kronecker delta.

The diagonal matrices $[\Lambda_s]$, $[\Lambda_c]$, $[\Lambda_\beta]$ and $[\Lambda_{k_x}]$, $[\Lambda_N]$ which corresponds to the spatial harmonics and the waveguide modes are defined as

$$[\Lambda_s] \;=\; \mathrm{diag}\{\sin(\beta_p d)\} \quad , \quad p = -\infty, \ldots, -1, +1, \ldots, +\infty \tag{59}$$

$$[\Lambda_c] \;=\; \mathrm{diag}\{\cos(\beta_p d)\} \quad , \tag{60}$$

$$[\Lambda_\beta] \;=\; \mathrm{diag}\left\{\frac{\beta_p}{k_0}\right\} \quad , \tag{61}$$

$$[\Lambda_{k_x}] \;=\; \mathrm{diag}\left\{\frac{k_{xq}}{k_0}\right\} \quad , \quad q = 0, \ldots, \infty \tag{62}$$

$$[\Lambda_N] \;=\; \mathrm{diag}\left\{\frac{1 + \delta_{0q}}{2}\right\} \quad . \tag{63}$$

The coupling integrals according to Eq. (55) are combined in the matrix $[C]$ for $p \neq 0$. Moreover it is useful to define a column vector $\boldsymbol{V}$ which consists of the complex conjugate of the coupling integrals between the zeroth order spatial harmonic and the qth waveguide mode:

$$\boldsymbol{V} = \begin{pmatrix} C_{00}^{*} \\ C_{01}^{*} \\ \vdots \\ C_{0q}^{*} \\ \vdots \end{pmatrix} \tag{64}$$

If we furthermore combine the field expanion coefficients $\mathcal{A}_m$ and $\mathcal{B}_n$ in the column vectors $\boldsymbol{\mathcal{A}}$ and $\boldsymbol{\mathcal{B}}$, respectively, and eliminate $\boldsymbol{\mathcal{A}}$ from Eqs. (54) and (58) we get the following linear system of equations for the determination of $\boldsymbol{\mathcal{B}}$:

$$\left([\Lambda_c]\,[\Lambda_\beta] + j\frac{L_0}{L}\,[C]\,[\Lambda_{k_x}]\,[\Delta]^{-1}\,[C]^{t*}\,[\Lambda_s]\right)\boldsymbol{\mathcal{B}} = -j\frac{L}{L_0}\,[C]\,[\Lambda_{k_x}]\,[\Delta]^{-1}\,q_0'\tilde{f}^{*}(k_0)\,\boldsymbol{V} \quad , \tag{65}$$

where the quadratic matrix $[\Delta]$ reads

$$[\Delta] = [\Lambda_N] + j\frac{L_0}{L}k_0 d\boldsymbol{V}\boldsymbol{V}^{t*}\,[\Lambda_{k_x}] \quad . \tag{66}$$

After solving Eq. (65) the amplitudes of the waveguide modes can be calculated from

$$\boldsymbol{\mathcal{A}} = -\,[\Delta]^{-1}\,[C]^{t*}\,[\Lambda_s]\,\boldsymbol{\mathcal{B}} - q_0'\tilde{f}^{*}(k_0)\,\boldsymbol{V} \tag{67}$$

and the expansion coefficient corresponding to the zeroth order spatial harmonic is finally given by

$$a_1 = j\frac{L_0}{L}k_0\boldsymbol{V}^{t*}\,[\Lambda_{k_x}]\,\boldsymbol{\mathcal{A}} \quad . \tag{68}$$

IV. Computation of the beam parameters

In this section it is shown how we can obtain the beam parameters from the results of the field analysis which has been presented in the previous section. There it has been assumed that the electromagnetic field is excited by a bunch with a shape described by a function $f(z - c_0 t)$ with respect to the axial coordinate. Hence it is possible to compute the electromagnetic field and subsequently the wakefield and the loss parameter.

Nevertheless it is more convenient to use $f(z - c_0 t) = \delta(z - c_0 t)$ as a source which makes the method modular in the following sense: Once we know the electromagnetic field for a delta-function excitation we can easily calculate the wakefield and the loss parameter for an arbitrary bunch shape without having to repeat the actual field analysis. In the following three subsections it is therefore demonstrated how these beam parameters can be calculated from the results of the field analysis for such an excitation.

IVa) Beam impedance

The beam impedance is defined as

$$Z(k_0) = \frac{1}{c_0}\int_{s=-\infty}^{\infty} W^{\delta}(s)\,e^{-jk_0 s}ds \quad , \tag{69}$$

where W^δ and s are the longitudinal wake function of a "point charge" and the usual wake coordinate in the negative z-direction emerging from the position of the exciting charge. For the wake function of an infinite periodic planar structure we have

$$W^\delta(s) = \frac{1}{q_0'} \lim_{z\to\infty} \frac{1}{2z} \int_{\xi=-z}^{z} E_z^{(1)}\left(d, \xi, t = \frac{s+\xi}{c_0}\right) d\xi \quad . \tag{70}$$

Note that W^δ according to the previous equation does not give the total change of momentum of a test particle which is actual infinite for our structure but its average value per unit length. Inserting the expression for W^δ of Eq. (70) into Eq. (69) yields

$$Z(k_0) = \frac{1}{q_0'} \lim_{z\to\infty} \frac{1}{2z} \int_{\xi=-z}^{z} \underbrace{\int_{\tau=-\infty}^{\infty} E_z^{(1)}(d, \xi, \tau)\, e^{-j\omega\tau} d\tau}_{\widetilde{E}_z^{(1)}(d,\xi,\omega)}\, e^{jk_0\xi} d\xi \quad , \tag{71}$$

where the inner integral represents the Fourier transformation of $E_z^{(1)}$. Substituting $\widetilde{E}_z^{(1)}$ by the corresponding field expansion series of Eq. (46) for the diffracted field, we obtain

$$Z(k_0) = \frac{Z_0}{q_0'} \left(\sum_{\substack{n=-\infty \\ n\neq 0}}^{\infty} \mathcal{B}_n \frac{\beta_n}{jk_0} \underbrace{\lim_{z\to\infty} \frac{1}{2z} \int_{\xi=-z}^{z} e^{jn\frac{2\pi}{L}\xi} d\xi}_{=0} + \frac{a_1}{jk_0} \underbrace{\lim_{z\to\infty} \frac{1}{2z} \int_{\xi=-z}^{z} d\xi}_{=1} \right) \quad . \tag{72}$$

It is obvious that the higher order spatial harmonics do not contribute to the beam impedance. Thus $Z(k_0)$ reads

$$Z(k_0) = \frac{Z_0}{q_0'} \frac{a_1}{jk_0} \quad . \tag{73}$$

Let us introduce the dimensionless quantity

$$\overline{\frac{a_1}{jk_0}} = \frac{1}{q_0'} \frac{a_1}{jk_0} \tag{74}$$

which is a_1/jk_0 normalized to the surface charge density q_0'. The computer code which has been implemented for the numerical evaluation of the presented method returns this value for the excitation of the zeroth order spatial harmonic. By making use of this quantity, we simply get for the beam impedance

$$Z(k_0) = \overline{\frac{a_1}{jk_0}} Z_0 \quad . \tag{75}$$

IVb) Wakefield

The wake for a bunch of particles which is characterized by the shape function $\lambda(s) = f(-s)$ can be calculated by the convolution of $\lambda(s)$ and $W^\delta(s)$:

$$W(s) = \int_{s'=-\infty}^{\infty} \lambda(s-s')\, W^\delta(s')\, ds' \tag{76}$$

Expressing $W^\delta(s)$ in the previous equation by the inverse Fourier transformation of the beam impedance and substituting $s - s'$ by ξ, we obtain

$$W(s) = \frac{c_0}{2\pi} \int_{k_0=-\infty}^{\infty} Z(k_0)\, e^{jk_0 s} \underbrace{\int_{\xi=-\infty}^{\infty} \lambda(\xi)\, e^{-jk_0\xi} d\xi}_{\widetilde{\lambda}(k_0)}\, dk_0 \quad , \tag{77}$$

where the inner integral is just the Fourier transformation of the bunch shape $\lambda(s)$. Consequently $W(s)$ is basically the inverse Fourier transformation of the beam impedance times the bunch spectrum:

$$W(s) = \frac{c_0}{2\pi} \int_{k_0=-\infty}^{\infty} Z(k_0)\, \tilde{\lambda}(k_0)\, e^{jk_0 s} dk_0 \tag{78}$$

Usually a Gaussian distribution is assumed for the bunch shape:

$$\lambda(s) = \frac{1}{\sqrt{2\pi}\sigma} e^{-\frac{1}{2}\left(\frac{s}{\sigma}\right)^2} \quad ; \tag{79}$$

and the corresponding spectrum reads

$$\tilde{\lambda}(k_0) = e^{-\frac{1}{2}(k_0\sigma)^2} \quad . \tag{80}$$

IVc) Loss parameter

The loss parameter per unit length k for an infinite periodic planar structure is defined as

$$k = -\frac{1}{(q_0')^2} \lim_{z\to\infty} \frac{1}{2z} \int_{\xi=-z}^{z} \int_{x=-\infty}^{\infty} \int_{t=-\infty}^{\infty} E_z(x,\xi,t)\, J_z(x,\xi,t)\, dt dx d\xi \quad . \tag{81}$$

The quantity k represents the averaged energy loss per unit length of a bunch of particles. Substituting E_z and J_z by the corresponding Fourier transformations and evaluating the integral in the x-direction leads to

$$k = -\frac{c_0}{2\pi\,(q_0')^2} \lim_{z\to\infty} \frac{1}{2z} \int_{\xi=-z}^{z} \int_{k_0=-\infty}^{\infty} \tilde{E}_z(d,\xi,k_0)\, \tilde{J}_z^*(d,\xi,k_0)\, dk_0 d\xi \quad . \tag{82}$$

Inserting the expression for J_z according to Eq. (43) into the above equation and making use of Eq. (71), we arrive at

$$k = -\frac{c_0}{2\pi} \int_{k_0=-\infty}^{\infty} Z(k_0) \left|\tilde{\lambda}(k_0)\right|^2 dk_0 \quad . \tag{83}$$

Thus the loss parameter is proportional to the integral extending over the entire frequency range from $k_0 = -\infty$ to ∞ of the beam impedance times the absolute value of the bunch spectrum squared.

V. Numerical results

Let us start the discussion of the numerical results checking the continuity conditions of the electromagnetic field at the grating interface ($x = 0$). In Fig. 6, the real parts of the normalized axial electric field corresponding to the diffracted and the waveguide field are compared. The agreement of both fields over the waveguide aperture ($0 < z < L_0$) is good. Furthermore the diffracted field vanishes for ($L_0 < z < L$) as it should be. From Fig. 6 it can also clearly be seen that the axial electric field tends to infinity at the waveguide edges ($z = 0$ and $z = L_0$) [14]. The strong oscillations of the curves are typical for a Fourier series representation of a discontinuous function [15]. This phenomenon even remains if we increase the number of expansion functions.

Fig. 7 presents the corresponding curves for the y-component of the magnetic field. The magnetic field is parallel to the edges of the parallel-plate waveguides and thus shows no singularities. Therefore the agreement between the diffracted and the waveguide field is almost

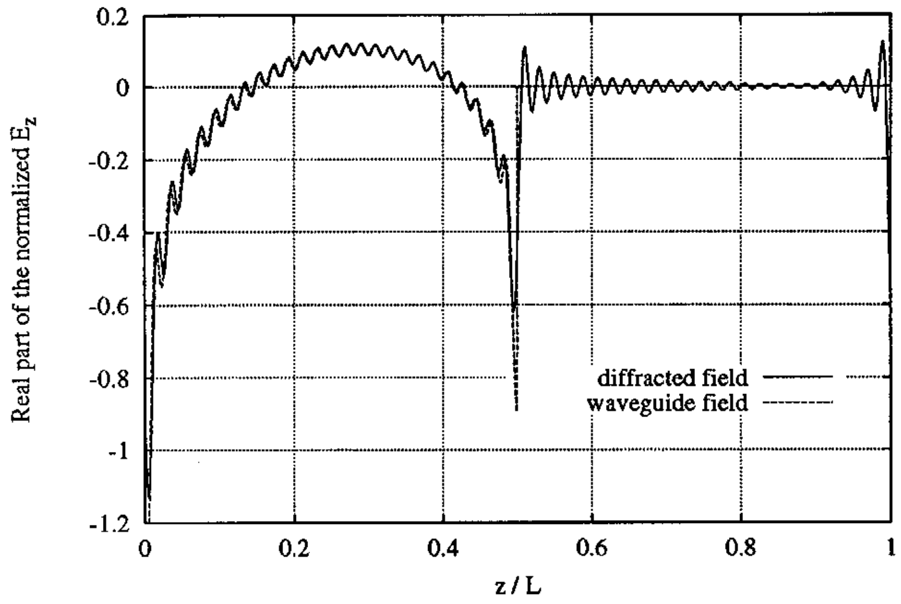

Figure 6: Comparison between the real part of the normalized E_z corresponding to the Rayleigh and the waveguide expansion. Parameters: $L_0 = 0.5L$, $d = L$ and $k_0 = 5/L$.

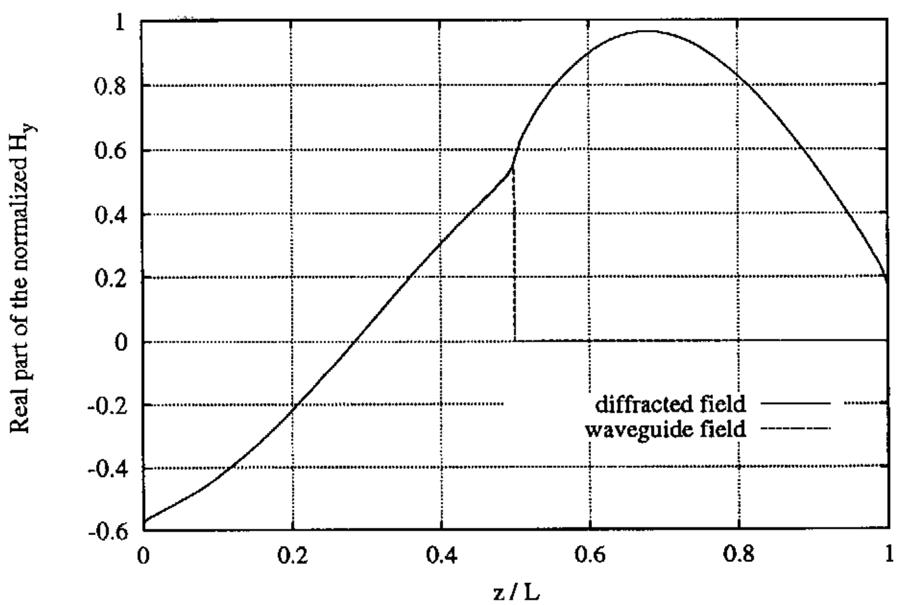

Figure 7: Comparison between the real part of the normalized H_y corresponding to the Rayleigh and the waveguide expansion. Parameters: see Fig. 6.

perfect. Note that in contrast to the axial component of the diffracted electric field the diffracted magnetic field does not vanish for $L_0 < z < L$. It is rather equal to the surface current density on the metal part of the grating interface.

Before we look at the beam parameters of periodic structures we have to remember that the mode matching technique has been applied to a planar structure. The relations between a circular configuration and its equivalent planar structure have been derived in Section II. There it has been shown how the beam impedance of a circular symmetric structure can be obtained from the analysis of a corresponding planar structure. Nevertheless we have to mark clearly to which geometry the presented numerical results belong.

Therefore let us briefly summarize the relations between the two classes of problems. If $Z_p^b(d = a/2)$ and $Z_c^{b\prime}$ denote the beam impedance of the planar two-layer structure where the distance between the sheet current and the grating surface is just one half of the radius of the corresponding corrugated beampipe and the beam impedance per unit length of the circular structure, repectively, then the relation

$$Z_c^{b\prime} = \frac{E_z|_{\rho=0}}{I_0} = \frac{1}{2\pi a} Z_p^b\left(d = \frac{a}{2}\right) \tag{84}$$

follows directly from Eqs. (17) and (35). From Eqs. (78) and (83) it is evident that similar relations also hold for the wakefields and the loss parameters:

$$W_c' = \frac{1}{2\pi a} W_p\left(d = \frac{a}{2}\right) \quad , \tag{85}$$

$$k_c' = \frac{1}{2\pi a} k_p\left(d = \frac{a}{2}\right) \tag{86}$$

The quantities corresponding to the circular and the planar structure are marked by the subscripts "c" and "d", respectively.

Fig. 8 shows the real part of the beam impedance for a planar grating as a function of frequency. The maximum normalized wavenumber which is $k_0L = 200$ corresponds to a frequency of about 10 THz for a period length of the grating of 1 mm. The beam impedance is calculated at 32768 frequency points and 200 spatial harmonics are taken into account. Even for this parameter set the cpu-time and memory requirements of the mode matching method are moderate due to its high numerical efficiency.

In the frequency range $0 \leq k_0L < \pi$ none of the higher order spatial harmonics is propagating with respect to the x-direction. Thus the beam impedance is a smooth function of k_0L. On the other hand the curve starts to oscillate rapidly at $k_0L = \pi$ for the following reason: According to Eq. (48) the spatial harmonic characterized by the index $n = +1$ turns from evanescent to propagating with respect to the x-direction at exactly this frequency which leads to standing wave effects between the magnetic wall and the grating interface. The spectral density of these resonances is very high because $d = 35\,\mathrm{mm} \gg L = 4/15$ mm. Nevertheless it can clearly be seen that the "pattern" of the curve changes every π where the number of spatial harmonics which propagate in the x-direction increases. Fig. 9 presents the beam impedance of a planar grating where the distance between the grating interface and the magnetic wall is even less than one grating period. In this case the spectral density of the resonances in the x-direction is therefore much less than in Fig. 8.

The frequency axis in Fig. 9 starts at $k_0L = 0$. From this figure it can clearly be seen that the beam impedance of a planar grating approaches a constant which is different from zero for $k_0L \to 0$. Note that a corresponding statement is also valid for a planar two-layer problem

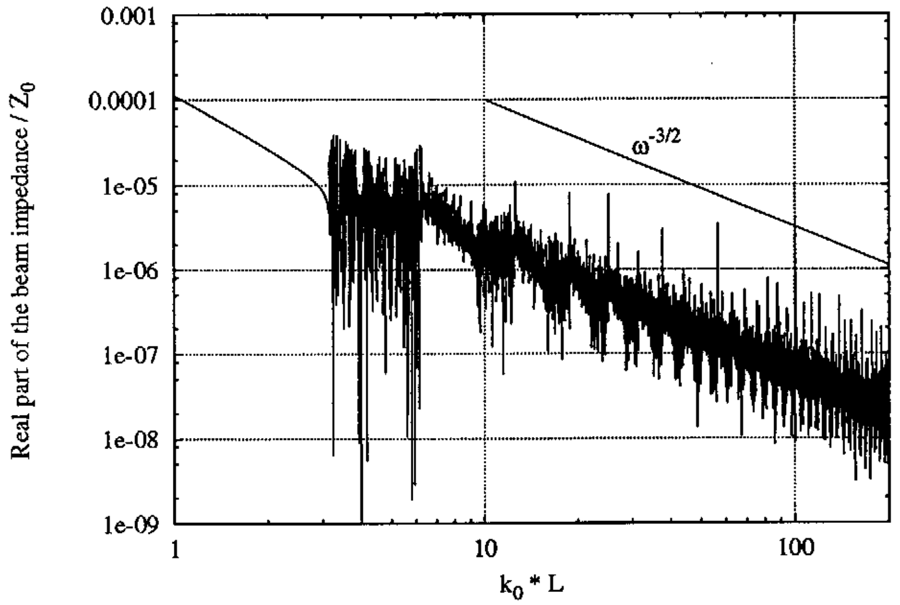

Figure 8: Real part of the beam impedance for a planar grating as a function of frequency. Parameters: $L = 4/15\,\mathrm{mm}$, $L_0 = 0.5L$ and $d = 35\,\mathrm{mm}$.

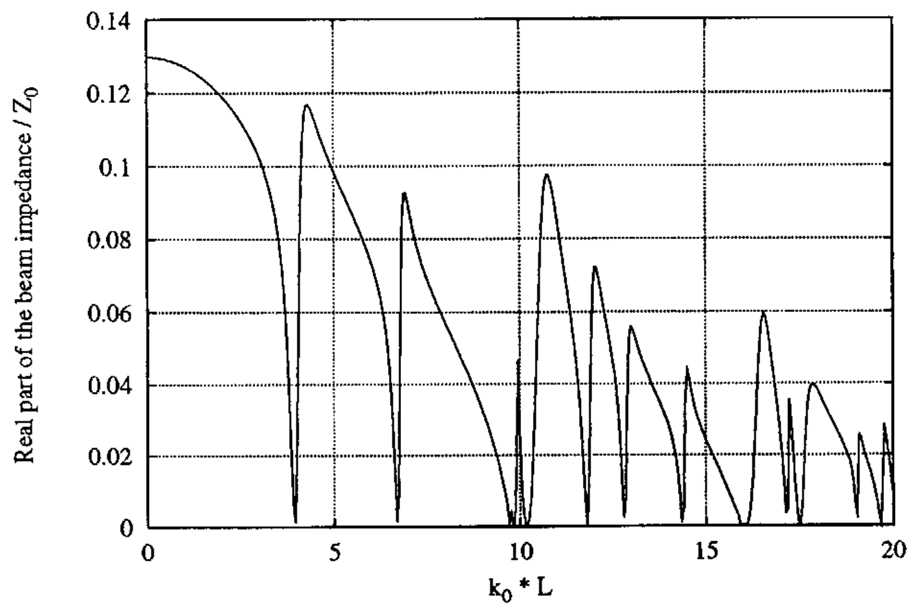

Figure 9: Real part of the beam impedance for a planar grating as a function of frequency. Parameters: $L_0 = 0.13L$ and $d = 0.5L$.

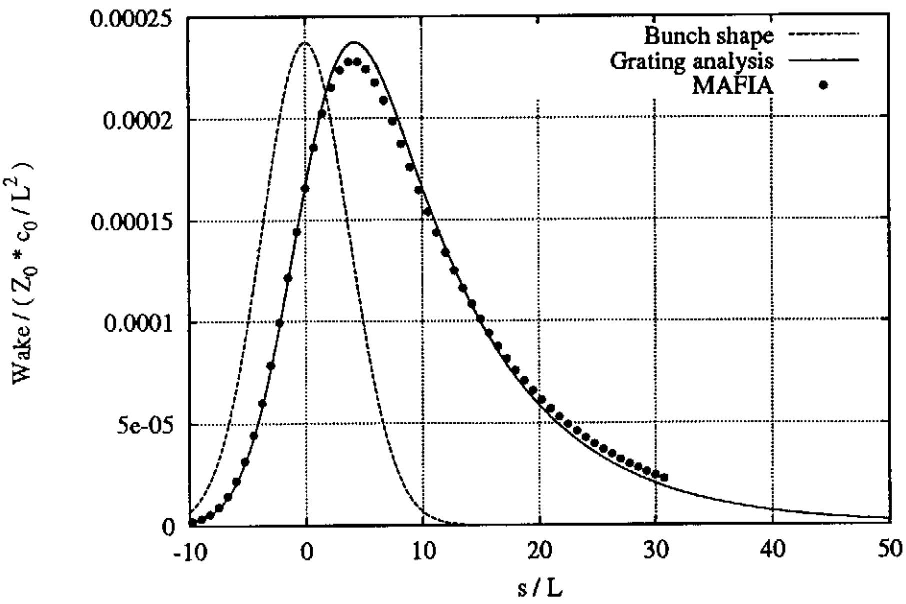

Figure 10: Comparison of the wakefields between the presented mode matching analysis and the MAFIA computer code. Parameters: $L = 4/15\,\mathrm{mm}$, $L_0 = 0.5L$, $a = 5\,\mathrm{mm}$ and $\sigma = 1\,\mathrm{mm}$.

which has already been found out in Subsection IIa). From the investigation of the dc case for the circular two-layer problem it is expected that the beam impedance of a corrugated circular beampipe vanishes at $k_0L = 0$. This statement is also supported by the results which are given in [16] where the beam impedance of two tubes connected by an infinite radial line has been calculated. Therefore we cannot use the planar structure as a model for the circular one for very low frequencies for which the large argument approximations of the Hankel functions is not valid.

In Fig. 8 a logarithmic scale is used for both axis. Thus a curve which is proportional to $\omega^{-3/2}$ corresponds to a straight line with a slope of $-3/2$ which is also given in this figure. From the two curves it can be concluded that the averaged beam impedance also drops as $\omega^{-3/2}$ which has already been shown in [3].

In Fig. 10 the wakefields corresponding to the presented mode matching analysis and the MAFIA computer code [17], [18] are compared. For the MAFIA calculations a corrugated circular beampipe with a length of 200 periods is assumed. The wakefield corresponding to the mode matching technique is obtained by scaling the result from the equivalent planar model according to Eq. (85). The agreement of the two wakefields is quite good which confirms the validity of the presented method.

The dependence of the wakefield on the bunch length is investigated in Fig. 11. The results which are presented in this figure are also obtained by transforming the results of an equivalent planar structure according to Eq. (85). The curves converge to an asymptotic wakefield corresponding to an infinitely small bunch length. For the given parameters the wakefield gets very close to the asymptotic curve ($\sigma/L = 0.1$) for a bunch length in the order of one grating period. Such an asymptotic wakefield has also been used in [9] where it is approximated by a special fit.

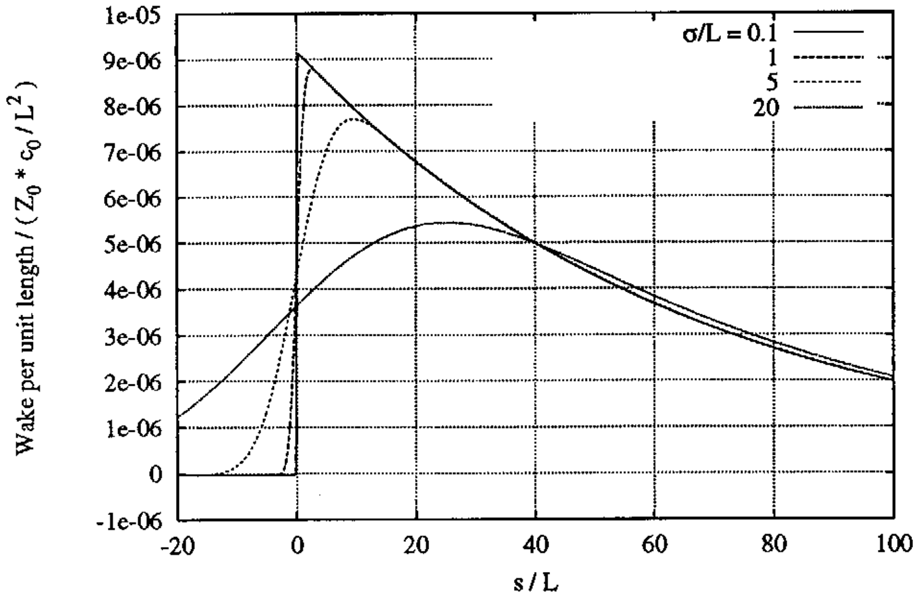

Figure 11: Dependence of the wakefield on the bunch length. Parameters: $L_0 = 0.5L$, $a = 262.5L$ and $k_m = 200/L$.

Fig. 12 presents the loss parameter per unit length as a function of bunch length for the same structure that has already been considered in Fig. 11. It indicates that the loss parameter approaches a constant for small values of σ/L whereas it begins to decrease significantly for bunches which are longer than one grating period.

In Fig. 13 the loss parameter of the accelerating structure of the S-Band Linear Collider (SBLC) [9] is presented as a function of bunch length. Each of the 6 m long sections of the SBLC consists of a constant gradient disk loaded structure with 179 cells plus one coupler cell. Although the iris radius is tapered in the original structure, we assume a constant iris radius ($a = 12\,\mathrm{mm}$) for our investigations. The results which are given in [9] are also based on this assumption. They are derived by making use of an asymptotic representation of the wakefields for short bunches. The agreement of the results corresponding to both methods is quite good. Nevertheless it seems to be that the mode matching technique yields a smaller limiting value of the loss parameter for very short bunches.

VI. Conclusions

The beam impedances of a circular and a planar two-layer problem have been calculated. The results have shown that the planar structure can be used as a model for the circular configuration if the parameters of the planar structure are properly chosen. Then the mode matching technique has been applied to compute the electromagnetic field excited by a bunch of ultra-relativisitic particles traversing a planar grating. It has been shown that the standard Rayleigh expansion which is usually used to represent the beam above the grating has to be modified for such an ultra-relativistic beam. It has been demonstrated how the beam impedance, the wakefield and the loss parameter can be obtained from the result of the field analysis. Due

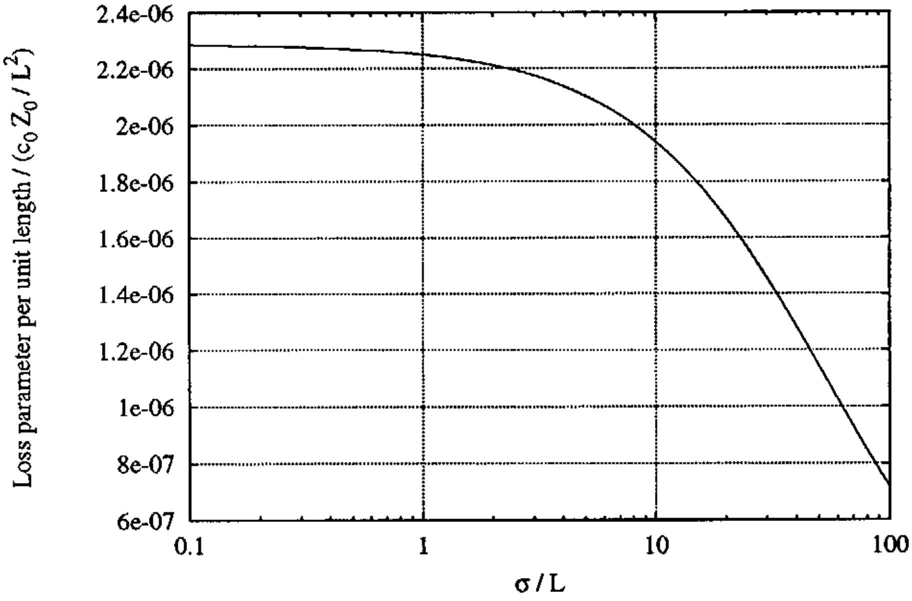

Figure 12: Loss parameter per unit length as a function of bunch length. Parameters: see Fig. 11.

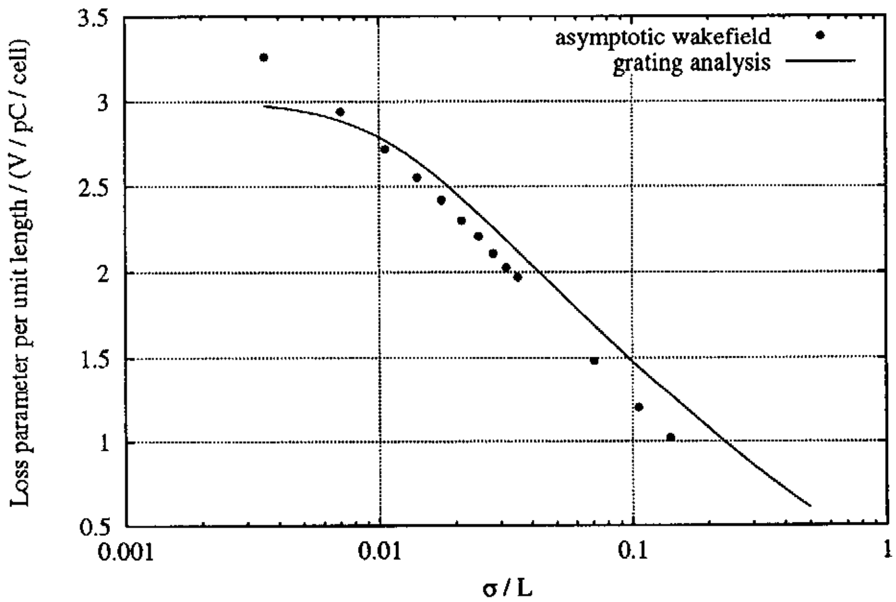

Figure 13: Comparison between the loss parameters calculated using the mode matching technique and those presented in [9] for the SBLC accelerating structure. Parameters: $L = 33.33\,\mathrm{mm}$, $L_0 = 0.85L$ and $a = 12\,\mathrm{mm}$.

to the equivalence of the circular and the planar two-layer problem it has been concluded that the calculated beam parameters are also approximately valid for a corresponding corrugated circular beam pipe. For various structures the beam parameters have been calculated. The validity of the presented mode matching technique has been checked by reference results which have been obtained using the electromagnetic field simulator MAFIA.

Acknowledgement

The authors are indebted to many colleagues from the S-Band linear collider study group and the TESLA collaboration who contributed to these ideas.

References

[1] M. Dohlus, N. Holtkamp and A. Jöstingmeier, "Design of a broadband absorber for $f >$ 100 GHz", *Meeting note: 26 Linear collider project meeting at DESY*, 1997.

[2] M. Dohlus, N. Holtkamp, A. Jöstingmeier, H. Hartwig and D. Trines, "Design of a HOM broadband absorber for TESLA", *Meeting note: 31 Linear collider project meeting at DESY*, 1998.

[3] S. A. Heifets and S. A. Keifets, "High-frequency limit of the longitudinal impedance of an array of cavities," *Phys. Rev. D*, vol. 39, pp. 961–970, 1989.

[4] G. V. Stupakov, "Coupling impedance of a periodic array of diaphragms", SLAC, SLAC-PUB-95-6802, 1995.

[5] A. Wexler, "Solution of waveguide discontinuities by modal analysis", *IEEE Trans. Microwave Theory Tech.*, vol. MTT-15, pp. 508–517, 1967.

[6] P. H. Masterman and P. J. B. Clarricoats, "Computer field-matching solution of waveguide transverse discontinuities", *Proc. IEE*, vol. 118, pp. 51–63, 1971.

[7] T. Itoh (ed.), *Numerical Techniques for Microwave and Millimeter-Wave Passive Structures*, John Wiley & Sons, 1989.

[8] H.-G. Unger, *Elektromagnetische Theorie für die Hochfrequenztechnik*, Hüthig, 1981.

[9] R. Brinkmann *et al.* (ed.), *Conceptual design of a 500 GeV e^+e^- linear collider with integrated X-ray laser facility*, DESY 1997-048, 1997.

[10] M. Dohlus, R. Lorenz, T. Kamps, H. Schlarb and R. Wanzenberg, "Estimation of longitudinal wakefield effects in the TESLA-TTF FEL undulator beam pipe and diagnostic section", DESY, TESLA-FEL 98-02, 1998.

[11] R. F. Harrington, *Time-Harmonic Electromagnetic Fields*, McGraw-Hill, 1961.

[12] H. Schlarb, *Resistive wall wake fields*, DESY, TESLA-FEL 97-22, 1997.

[13] R. E. Collin, *Foundations for Microwave Engineering*, McGraw-Hill, 1966.

[14] R. E. Collin, *Field Theory of Guided Waves*, IEEE PRESS, 1991.

[15] J. van Bladel, *Electromagnetic Fields*, Springer Verlag, 1985.

[16] H. Henke, "Point charge passing a resonator with beam tubes", *Archiv für Elektrotechnik*, vol. 69, pp. 271–277, 1986.

[17] T. Weiland, "On the numerical solution of Maxwell's equations and applications in the field of accelerator physics", *Particle Accelerators*, vol. 15, pp. 245–292, 1984.

[18] The MAFIA collaboration, *User's Guide MAFIA Version 3.2*, CST GmbH, Lauteschläger-str. 38, D64289 Darmstadt.